Basic Principles of Magnetic Resonance Imaging—An Update

ANN L. SCHERZINGER, PhD, *Denver, and* WILLIAM R. HENDEE, PhD, *Chicago*

Magnetic resonance (MR) imaging technology has undergone many technologic advances over the past few years. Many of these advances were stimulated by the wealth of information emerging from nuclear magnetic resonance research in the areas of new and optimal scanning methods and radio-frequency coil design. Other changes arose from the desire to improve image quality, ease siting restrictions and generally facilitate the clinical use of MR equipment. Many questions, however, remain unanswered. Perhaps the most controversial technologic question involves the optimal field strength required for imaging or spectroscopic applications or both. Other issues include safety and clinical efficacy. Technologic issues affect all aspects of MR use including the choice of equipment, examination procedure and image interpretation. Thus, an understanding of recent changes and their theoretic basis is necessary.

(Scherzinger AL, Hendee WR: Basic principles of magnetic resonance imaging—An update, *In* High-tech medicine [Special Issue]. West J Med 1985 Dec; 143:782-792)

The first nuclear magnetic resonance image was produced by Lauterbur in 1973[1]; since that time, magnetic resonance (MR) imaging has evolved into a clinically useful, although not yet widespread, imaging tool in diagnostic medicine. In early 1985, at least 200 MR imaging units were operating worldwide, with 70% of the total in the United States. Most of the initial sites were university based, but many of the more recent installations have been in outpatient clinics and independent diagnostic centers. Magnetic resonance imaging units are available from 18 manufacturers,[2] with magnetic field strengths ranging from 0.04 to 2 tesla. Two MR imaging societies have a combined enrollment of 1,500 members and several journal articles on MR imaging are published each month.

The rapid growth in clinical applications has been accompanied by numerous technologic advances in MR imaging over the past few years. These advances have affected imaging techniques, image quality, siting considerations, safety concerns and several other aspects of the clinical applications of MR imaging. Still, many questions remain unanswered, such as the clinical efficacy and cost effectiveness of the clinical applications of MR imaging, the optimum magnetic field strength for imaging, long-term health implications of exposure to intense magnetic fields and the overall fiscal viability of the modality.

Imaging Techniques

The basic principles of MR imaging are discussed in several articles.[3-5] Some of these articles describe the two most commonly used imaging sequences, spin echo and inversion recovery, together with modifications of these sequences that have yielded improvements in the signal-noise ratio, contrast resolution and imaging time. Multislice, multiecho spin-echo imaging has become the major MR imaging technique used for clinical imaging; a standard spin-echo examination includes one set of spin-lattice relaxation time (T1)-weighted images (short repetition time [TR]) and one set of spin-spin relaxation time (T2)-weighted images (long TR).

The spin-echo pulsing technique is shown in Figure 1. In this technique, a 90° pulse is applied to a selected slice of tissue. In response, a free induction decay (FID) signal is induced in the receiver coil with an initial value that is proportional to the longitudinal magnetization of the sample at the time of the pulse. The signal decays with a time constant T2*, which reflects both spin-spin relaxation (time constant T2) and relaxation caused by nonuniformities in the static magnetic field. At a time (TE2) following the 90° pulse, a 180° pulse is applied. This pulse reverses the signal decay caused by inhomogeneities in the field, and an echo signal is produced at a time TE following the 90° pulse. The amplitude of this echo relative to the initial value of the FID is a function of

From the Division of Radiological Sciences, Department of Radiology, University of Colorado Health Sciences Center, Denver. Dr Hendee is now Assistant Vice-President for Science and Technology, American Medical Association, Chicago.

Reprint requests to Ann L. Scherzinger, PhD, Department of Radiology, A034, University of Colorado Health Sciences Center, 4200 E 9th Ave, Denver, CO 80262.

ABBREVIATIONS USED IN TEXT

AC = alternating current
CT = computed tomography
FDA = Food and Drug Administration
FID = free induction decay
Gd-DTPA = gadolinium-diethylenetriaminepentaacetic acid
MR = magnetic resonance
T1 = spin-lattice relaxation time
T2 = spin-spin relaxation time
T2* = T2 and relaxation caused by nonuniformities in static magnetic field
TE = echo time
TR = repetition time

the true spin-spin relaxation time, T2, and the echo delay time TE. After a time, TR, the entire spin-echo sequence is repeated. A long TR (longer than T1) is chosen if one wishes to allow all tissues to undergo complete longitudinal relaxation. The signal intensity following the 90° pulse is then independent of T1 because the imaged tissue was fully relaxed before the 90° pulse was applied. If the TR is shortened, the tissue will not have complete longitudinal relaxation, the signal intensity will vary with T1 and the image will contain some T1 weighting. Within this framework, the TE values can also be changed to alter the T1 and T2 weighting of the image.

The optimum values of TE and TR for imaging specific tissues is still relatively uncertain, even though considerable theoretical and experimental work has been directed towards answering this question.[6-8] To eliminate the need for a priori knowledge of the appropriate pulse sequence, techniques have been developed to calculate images for any assembly of characteristics from data obtained at two different spin-echo sequences.[9,10] These images have been shown to correlate well with those acquired using actual pulse sequence.

Multiecho spin-echo images are produced by injecting 180° pulses at times TE, 2 TE, 3 TE and so forth following the initial 180° inversion pulse (Figure 2). From two to eight multiple echoes can usually be obtained, with the signal becoming weaker with each subsequent echo, as shown in Figure 2. Thus, the signal-noise ratio is a dominant factor in choosing the number of multiple echoes used for imaging. Since no one combination of TE and TR provides optimal viewing for all tissue types, this technique is used to provide images with a range of T1 and T2 weighting (multiple TE values).

Multislice imaging techniques have been developed to decrease patient examination time. In the standard spin-echo technique, TE is much shorter than TR—that is, 15 to 100 ms compared with 0.5 to 5 seconds—where a long TR is required to permit T1 relaxation of the sample slice before initiating the next imaging sequence. During this waiting period, adjacent slices of tissue can be imaged, as shown in Figure 3. Thus, the interleaving technique of multislice imaging permits acquisition of images from several slices during the time otherwise required to image only one slice. The number of slices constituting a multislice imaging procedure depends on the value of TR used.

The time saved can be illustrated by the equation for the imaging time, T, for a single slice:

$$T = TR \times n \times N$$

Here n is the number of imaging sequence acquisitions required per projection—that is, the number of averages plus one—and N is the number of measured projections—that is, the image matrix size. Thus, a single 256 × 256 slice with TR equaling two seconds and one average slice (two acquisitions) would take 17 minutes to acquire. Multislice techniques can provide as many as 20 such images in that amount of time. Producing multislice, multiecho images reduces to 12 the number of slices obtained for a four-echo sequence using the values above. Additional time savings can be achieved by improving the signal-noise ratio so that the number of imaging sequences, n, required can be reduced. Techniques being developed that use radio-frequency pulses to force T1 relaxation and thus reduce TR will also reduce scan times.

The multislice imaging technique, although simple in concept, introduces a variety of practical difficulties. Ideally, a

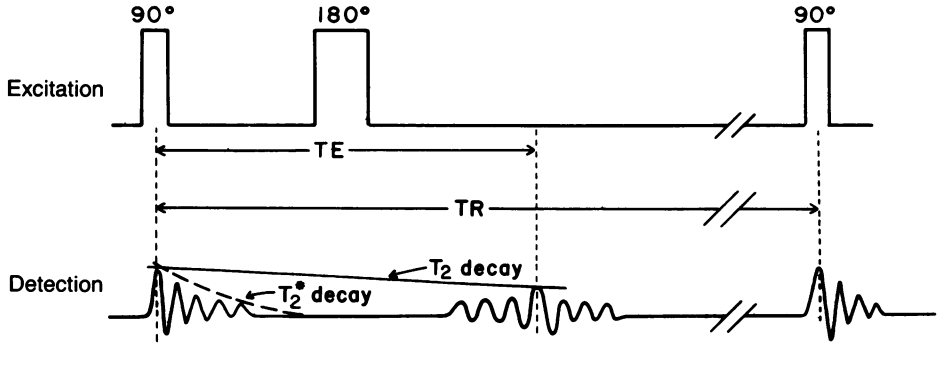

Figure 1.—Radio-frequency pulsing scheme and signals detected from a spin-echo pulse sequence. T2 = spin-spin relaxation time, T2* = spin-spin relaxation time and relaxation caused by nonuniformities in static magnetic field, TE = echo time, TR = repetition time

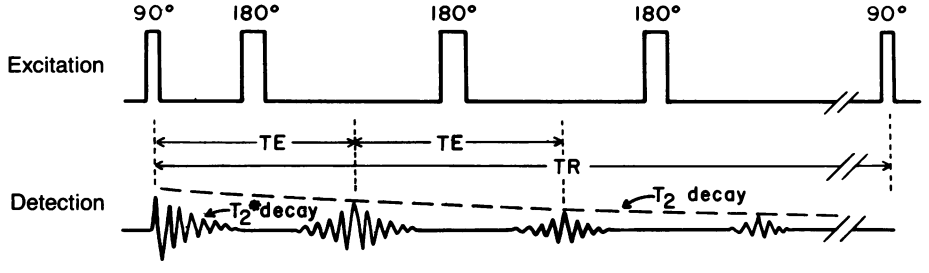

Figure 2.—Radio-frequency pulsing scheme and signals detected from a multiecho spin-echo pulse sequence. The symbols are as given in Figure 1.

sequence of adjacent images through the tissue volume of interest is desired, with no gaps of unimaged tissue and no overlap between slices. This objective is difficult to achieve, however, because the gaussian distribution of frequencies in the radio-frequency pulse causes excitation of tissue on either side of the desired slice (Figure 4-A). To avoid problems caused by the poorly defined borders of the tissue slices, multislice techniques traditionally provide images separated by gaps of unimaged tissue, with the gaps ranging from 3 to 10 mm.

Techniques have been devised to minimize the gaps between adjacent tissue slices. In one technique, an optimization approach is used to order the sequence of excited slices.[11] Another approach relies on two multislice acquisitions, with the second designed to produce images in the tissue regions constituting the gaps in the first acquisition. With a third technique, the radio-frequency pulse is tailored to provide a square, rather than gaussian, frequency profile, as shown in Figure 4-B. In this case, the radio-frequency pulse, $1f(t)$, is modulated by a sinc function, sinx/x, to give the radio-frequency pulse envelop shown in Figure 4-B. The result is a square frequency profile, $f(w)$, to define the slice. This technique requires rapid switching of the gradient fields making it more difficult to use at high field strengths.

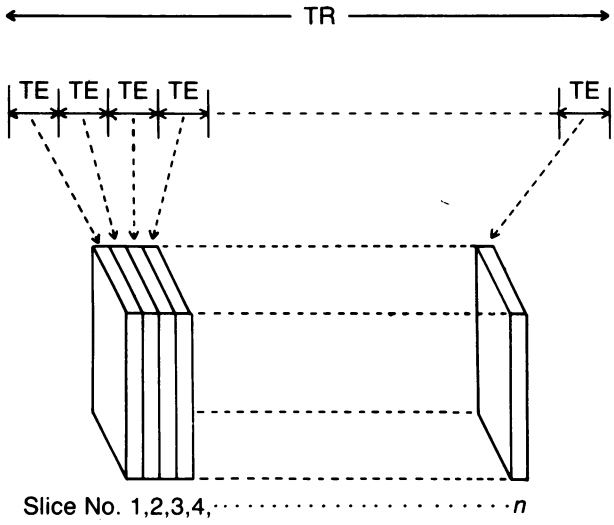

Figure 3.—Multislice imaging technique. The echo time (TE) span includes time to excite nuclei and record echo(es). TR = repetition time, n = number of imaging sequences

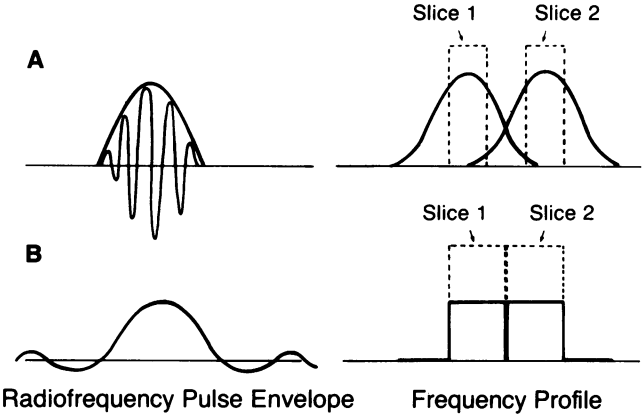

Figure 4.—Slice selection techniques: **A,** a typical gaussian radio-frequency pulse produces slices with overlap or gaps, or both. **B,** A sinc radio-frequency pulse produces slices with no overlap or gaps.

Volume imaging methods require considerable time and generate extensive data; hence, they are not used routinely.[12] Volume imaging techniques have one advantage, however, in that they do not produce slice overlap and gap problems as the entire volume of tissue is sampled simultaneously. Hence, these techniques have been used to provide thin, adjacent images, such as 0.9 mm slices with no gap, of small anatomic regions such as the pituitary[13] and heart.[14]

Conventional multislice spin-echo techniques have been modified to provide information about specific aspects of tissue pathology. Most hydrogen in tissue is present in water or in the long carbon chains of fat triglycerides. In fat, the hydrogen nuclei have a different chemical environment from that in water; consequently, the local magnetic fields are different and the Larmor frequency for hydrogen in water is shifted slightly from the frequency for hydrogen in fat. This chemically induced shift (termed a "chemical shift") is present as an artifact in conventional high-field images.[15] A chemical shift of 3.5 ppm for the hydrogen nuclei of fat and water is shown in Figure 5-A, where the units of chemical shift are stated as parts per million of the Larmor frequency of hydrogen in water. When stated in these units, the chemical shift is independent of field strength and is related to the actual shift in frequency by the expression

$$\Delta W = \delta \times W_L$$

where δ is the chemical shift (ppm) and W_L is the reference Larmor frequency. At 0.35 tesla ($W_L = 15$ MHz), the water and fat peaks are shifted by 53 Hz, whereas at 2 tesla ($W_L =$ 84 MHz), the same peaks are separated by 294 Hz. It is this

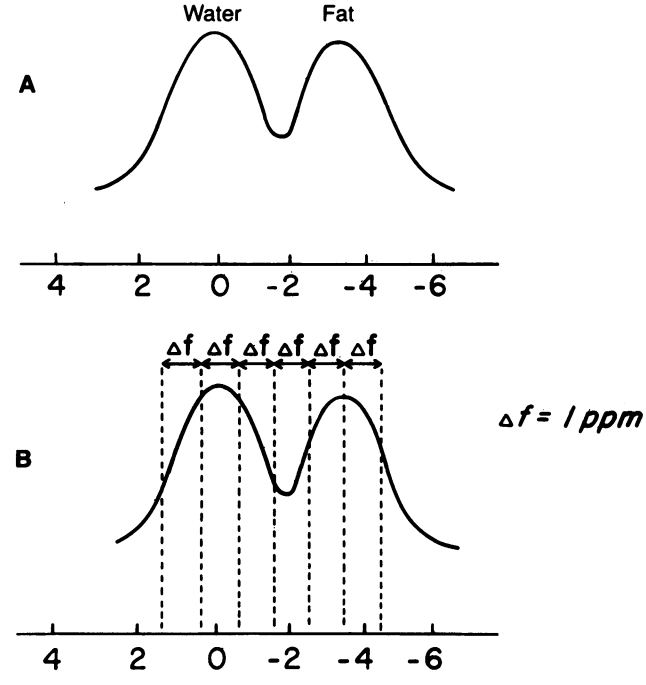

Figure 5.—Proton spectra of tissue at fields less than 2 tesla. The horizontal axis represents a chemical shift with respect to the water peak in units of parts per million of the Larmor frequency of hydrogen in water (see text). **A,** Proton spectra and **B,** slices obtained with a resolution of 1 ppm by the 3-dimensional Fourier transform technique of Pykett and Rosen.[16]

larger shift at higher frequencies that produces an artifact when imaging at higher field strengths.

Chemical shift imaging techniques, employing a modified form of the conventional spin-echo sequence, have been used to obtain separate images of water and fat distributions in tissue at field strengths as low as 0.15 tesla.[17,18] Two imaging sequences are required with this approach to obtain four sets of images: fat plus water, fat and water difference, fat only and water only. Images are obtainable within the same time and resolution constraints as conventional spin-echo techniques. With higher field systems, a three-dimensional Fourier transform technique can be used to obtain images of the signal intensities of the hydrogen spectral peaks at a separation of 0.1 ppm. For fat and water, separate images can be obtained at several positions in the hydrogen spectrum as shown in Figure 5-B. If desired, peaks in the water or fat range can be summed to yield a total water or total fat image.[16] A third technique involves obtaining a water image by saturating the fat resonance before conducting a traditional spin-echo two-dimensional Fourier transform imaging sequence. To illustrate, the fat resonance can be irradiated with a 90° pulse before beginning the normal imaging sequence by a radio-frequency pulse at the resonant frequency of fat. When combined with the first 90° pulse of a traditional spin-echo imaging sequence, the fat resonance will have undergone a 180° flip, making its signal invisible to the MR receiver coil.

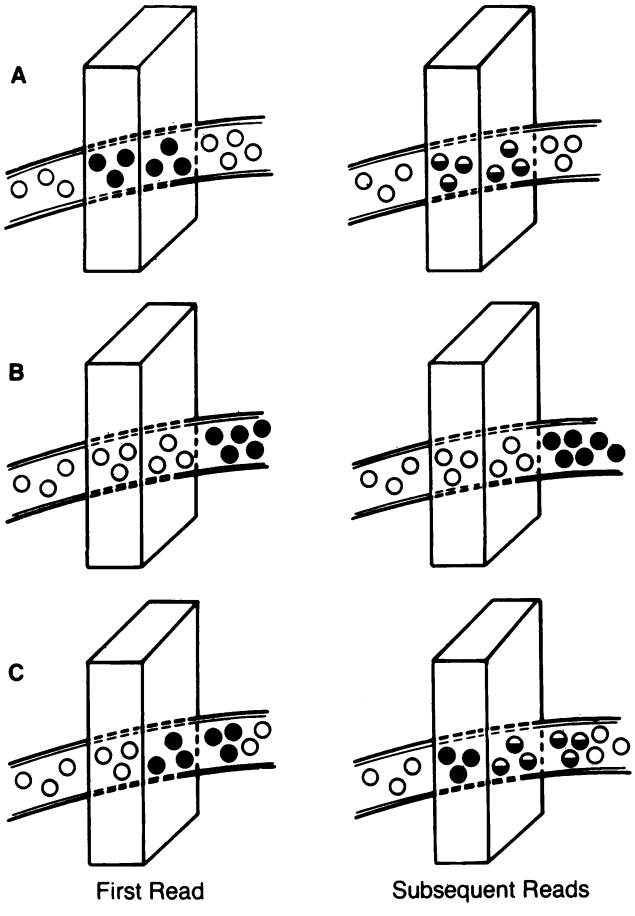

Figure 6.—This diagram shows the effect of blood flow on the magnetic resonance image intensity: **A,** Stationary blood, **B,** fast-flowing blood and **C,** slow-flowing blood.

Conversely, a fat image can be obtained by first saturating the water peak.[19] At present, chemical shift imaging is an experimental technique; images have been useful, however, in showing fatty infiltration of the liver.[20]

Another anomaly of conventional imaging is the influence of blood flow on signal intensity in vascular structures.[21] As an illustration, stationary blood would be expected to behave like tissue in terms of magnetic resonance imaging. In a spin-echo sequence, the initial radio-frequency pulse produces a maximal signal, with negligible relaxation occurring between the 90° pulse and the measurement of the radio-frequency signal. But, if a TR is chosen so that the nuclei remain partially saturated—that is, not completely relaxed—for all subsequent 90° pulses, the resulting signal intensity is diminished, as diagrammed in Figure 6-A.

For fast-moving blood (10 cm per second or faster),[21] protons initially excited by the radio-frequency pulse move out of the image plane before the signal is measured, as shown in Figure 6-B. Blood moving into the image plane has not been exposed to a radio-frequency pulse and hence yields no signal. In the image, fast-moving blood is shown as a dark, signal-less region.

With slow-moving blood, these two events are combined to provide a signal greater than that from either stationary or fast-moving blood. During the repetition time, the partially saturated blood remaining from the previous sequence is replaced in part by blood flowing into the imaging plane. The subsequent 90° radio-frequency pulse elicits a stronger signal from this new blood (Figure 6-C) than from the remaining partially saturated blood and the total signal is enhanced over that of stationary blood. This effect is referred to as "paradoxical enhancement" and yields a bright area in regions of the image representing slow-moving blood. Slow flow can also be distinguished by a distinct rephasing effect on even echoes of a multiecho imaging sequence.[22] Because of these flow effects, information about flow velocities can be elicited by appropriate manipulation of the image sequence variables TE and TR.[23,24] Recent studies suggest that flow measurements from imaging techniques may depend also on other aspects of the measuring technique, such as the reconstruction algorithm.[25]

Image Quality

As in any imaging modality, image quality is a subjective characteristic; nevertheless, certain image variables can be measured as an indication of image quality. These variables include the ratio of signal to noise, the ratio of contrast to noise, spatial resolution, the presence (or absence) of artifacts and the accuracy of T1 and T2 values determined from the image. To date, quantifiable standards have not been developed for an overall evaluation of the quality of magnetic resonance images; hence, vendors tend to emphasize the image variables at which they excel.

For an MR image, the signal-noise ratio is commonly described by the equation

$$S\text{-}N = (I_T - I_B)/\sigma_B$$

where I_T and I_B are the signal intensities of the tissue of interest and the image background, and σ_B is the standard deviation of the background signal. The signal-noise ratio depends strongly on the pulse sequence and pulsing times used for

imaging. For example, it is obvious from Figure 2 that the signal I_T from the tissue depends on which echoes are used to form the image and that the background signal is constant. Values of signal-noise ratio ranging from 10 to 100 are frequently quoted[26,27]; these values are obtained at different pulse sequences and pulsing times, however, and it is difficult to compare the signal-noise specifications from one vendor to another. Signal-noise values are often quoted in association with the field strength issue discussed below but these quotations frequently shed little light on the issue.

The contrast-to-noise ratio is similar to that of signal to noise, except that it is used to measure the difference in signal, and thus the visibility, of two different tissues of interest, such as gray and white matter or tumor and normal tissue. The contrast-noise ratio is described by the expression[5]

$$C\text{-}N = (I_{Ta} - I_{Tb})/(I_0\sigma_B)$$

where I_{Ta} and I_{Tb} are the signal intensities of the two tissues of interest. I_0 is the maximal signal measurable for the two tissues—that is, the signal obtained after a single 90° pulse is applied following complete longitudinal relaxation of the tissue—and σ_B is the standard deviation of the background. If the spin densities of the two tissues are equal, they should have the same value for I_0 irrespective of the imaging regimen used; I_{Ta} and I_{Tb} are not independent of the selected imaging regimen, however. Hence, the maximal contrast-noise ratio is often used to predict the optimal pulse sequence for imaging specific tissues.[6]

Both the signal-noise and contrast-noise ratios affect the spatial resolution of the magnetic resonance image. Values for the spatial resolution are often quoted, inappropriately, as the predicted picture element (pixel) size of the image. That is, for an anatomic region of 30 cm by 30 cm, a 128×128 image will provide a pixel size of 2.3 mm; for a 256×256 image of the same object, the pixel size will be 1.15 mm.

An increase in matrix size to decrease pixel size requires a dramatic increase in imaging time, as N increases in the expression for imaging time presented earlier. Slice thickness can be reduced in an effort to decrease partial volume effects and to improve resolution. With reduced slice thickness, however, more slices are needed to encompass a given volume of tissue, and the imaging time increases. As is apparent from these examples, there is almost always a trade-off between spatial resolution and imaging time.

In actuality, the signal-noise ratio provides a practical limit to the effective spatial resolution. The borders of a volume element of tissue (voxel) are defined by the pixel size and the slice thickness. As the voxel size is reduced, there are fewer resonating nuclei present in the voxel, causing a reduction in the measured signal and a decrease in signal-noise ratio. This decrease places a practical limit on the spatial resolution obtainable with an MR imaging unit.

Motion artifacts occur in MR imaging principally because of the length of time required to obtain a set of MR images. These artifacts are especially apparent in images of the thorax and upper abdomen.

Cardiac studies with MR imaging can be gated to the R wave and the electrocardiogram to decrease motion artifacts; detailed images of as many as ten sections obtained at one to five different times during the cardiac cycle have been published.[14] One disadvantage of cardiac gating is that the TR interval depends on the pulse rate. Consequently, the TR cannot be easily manipulated; in fact, TR is never constant as the pulse rate is often variable. This variability interferes with computing of the tissue relaxation characteristics, T1 and T2.

Gated cardiac images can be obtained with either multislice or volume imaging techniques. Unless a special sequencing procedure is used, however, multislice techniques yield images of sequential slices at different times in the cardiac cycle, because the slices cannot be taken simultaneously. Volume imaging techniques require longer times for acquiring data, but they can provide slices produced at the same time in the cardiac cycle. Presently, cardiac images are produced in the standard orthogonal planes. Techniques are being developed, however, to produce images in oblique planes that correlate more closely with conventional radiography.[28-30]

Images of the upper abdomen often contain artifacts caused by respiratory motion. The respiratory cycle is not constant in either depth or length, and gating of respiratory motion is difficult. Gross motion artifacts have been removed by respiratory gating, but at the cost of a 1.5 to 2 times increase in imaging time, depending on the characteristics of the respiratory cycle.[31]

Motion artifacts can also be eliminated by the use of the echo planar imaging technique.[32] This technique uses an oscillating gradient field to localize the signal in the traditional phase encoding plane of a normal two-dimensional Fourier transform imaging method.[5] In contrast to this traditional imaging method, a separate data collection sequence for each of N pixels in the phase encoding direction is not required. Scan times are reduced to 10 to 100 ms per slice because all of the image data for one planar slice are obtained from one pulsing sequence. To date, echo planar imaging has been used primarily for the thorax, where 32 slices with 16 images per slice at 16 phases of the cardiac cycle have been produced (512 images total).[33] A typical examination is completed in four to eight minutes, depending on a patient's cardiac period. Because of signal constraints, these images have only 32×32 pixel resolution (6 mm) and a slice thickness of 8 mm. To date, echo planar imaging has been done only at low fields (0.1 tesla); the technique requires the rapid switching of gradient magnetic fields, and it is uncertain whether it will be feasible at higher field strengths. To overcome this difficulty, hybrid techniques involving a combination of two-dimensional Fourier transform and echo planar imaging are being investigated.

Another measure of image quality is the accuracy of T1 and T2 values calculated from the image. In 1971, Damadian[34] suggested that normal and malignant tissue may be distinguishable on the basis of differences in their T1 values. Subsequent conflicting reports have appeared concerning the value of T1 and T2 as tissue-specific indicators.[35-37] Much of the conflict has been attributed to inaccuracies in the T1 and T2 values extracted from images. These inaccuracies arise from the numerous errors inherent in the measuring technique.[38,39] These include high noise levels, effects of flow and motion, partial volume effects, slice overlap and nonuniform excitation of slices. Recent reports, however, have shown accuracies of 96% to 98% in measured T1 and T2 values for a few types of tissues and test solutions.[40,41]

Contrast Agents

The contrast in a magnetic resonance image is a reflection primarily of differences in T1 and T2 relaxation times among

various tissues. By using in vivo contrast agents to selectively alter the relaxation times, image contrast often can be improved. Contrast agents currently under investigation are principally paramagnetic materials. These substances have large magnetic moments resulting from the presence of unpaired electrons in the atomic structure. The presence of a paramagnetic substance alters the magnetic field in the immediate vicinity of the substance. This alteration facilitates relaxation and shortens T1 and T2 relaxation times.[42,43]

Paramagnetic agents investigated to date have primarily been complexes and salts of the transition metals and rare earth elements, including manganese, iron, cobalt, nickel. copper, chromium and gadolinium. Intravenous injections of manganese chloride have altered the T1 values of abdominal organs.[44] Recent studies have contradicted earlier reports of the high toxicity of this material.[45] Manganese has also been complexed to a monoclonal antibody in an attempt to provide better delineation of myocardial infarction.[46]

Weak Geritol solutions containing ferrous ammonium citrate can be used as a nonhazardous orally administered contrast agent to enhance the image of the gastrointestinal tract.[47] Recently an iron complex, iron (III) ethylene *bis*-(2-hydroxyphenylglycine) or Fe(EHPG), has been shown to enhance the imaging of normal liver parenchyma without adverse effects in rats.[48]

One of the more promising contrast agents is a complex of gadolinium (Gd) with diethylenetriaminepentaacetic acid (DTPA).[49,50] Administered intravenously, Gd-DTPA is used as an indicator of organ perfusion[51] and has been compared in behavior with the iodinated contrast agents used in computed tomography (CT).[52] Gd-DTPA has been effective clinically in enhancing the images of brain tumors,[53] brain abscesses[54] and ischemic myocardial tissue.[55,56] Early studies have shown no toxicity of the agent[45] and it is currently undergoing phase III trials in humans in four institutions.

Nitrogen-stable free radicals are another class of contrast agents under investigation. Free radicals are paramagnetic because they possess an unpaired electron in the valence molecular orbital.[42,43] Nitrogen-stable free radicals have been shown to enhance the imaging of renal[57] and brain[58] tissues; toxicity studies are ongoing.

Radio-frequency Coils

Recent improvements in MR image quality are attributable in part to design improvements in radio-frequency coils. To illustrate, a saddle-shaped radio-frequency coil is placed inside a solenoidal magnet as shown in Figure 7. If an alternating current (AC) is transmitted through the coil, an alternating B_1 field is generated perpendicular to B_0, the static magnetic field, and the coil acts as a transmitter. Conversely, if an oscillating magnetic field produced by precessing nuclei in the plane perpendicular to B_0 is sensed by the coil, a current is generated in the coil and the coil acts as a receiver.

A radio-frequency coil is often represented as a series LRC circuit, where L is the circuit inductance, R is the resistance and C the capacitance.[59] The coil is most sensitive to the magnetic resonance signal when the AC frequency of the circuit, given by

$$f = (2\pi)^{-1}(LC)^{-1/2},$$

is tuned to the Larmor frequency. In this condition, the coil will provide the largest MR imaging signal in response to the precessing nuclei. When a body (a load) is placed in the coil, additional inductance and capacitance are encountered, thus altering the optimal receiving frequency of the coil from that of its unloaded state. Most MR imaging systems permit fine tuning of the coil frequency to obtain the maximum signal with the patient in place.

Any radio-frequency coil is sensitive to a range of frequencies, Δf, about the center Larmor frequency. This range of frequencies—the bandwidth—is described by the coil Q, where a high Q means a narrow bandwidth, as shown in Figure 8. A high Q coil is preferred because it limits the amount of noise detected by the coil. When a body is placed in the coil, Q is decreased significantly below its unloaded value, with the decrease dependent on the tissue volume encompassed by the coil.

Coil geometries are determined by the desire to provide homogeneous radio-frequency fields for irradiating and measuring samples and to maximize the amount of tissue located in the radio-frequency field. This latter factor is referred to as the filling factor of the coil, and a higher filling factor provides a stronger signal. Typical coil arrangements include solenoid coils in permanent magnet systems and saddle-shaped coils in resistive and superconducting magnet systems. At high fields (greater than 1 tesla), the coil geometries have to be modified extensively because the coil length becomes comparable with the radio-frequency wavelength and phase shift artifacts occur.[60]

Finally, coil optimization includes eliminating other

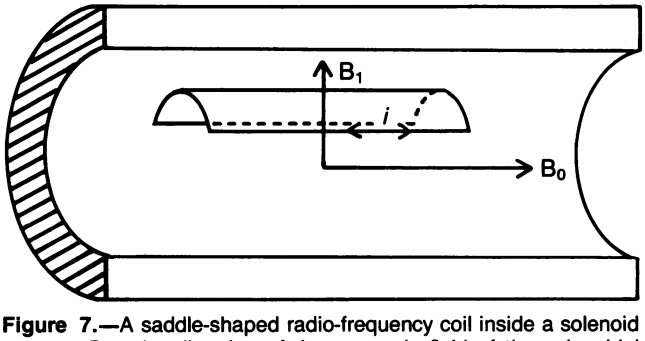

Figure 7.—A saddle-shaped radio-frequency coil inside a solenoid magnet. B_0 = the direction of the magnetic field of the solenoidal magnet, B_1 = the direction of the magnetic field produced by current flow, *i*, in the radio-frequency coil.

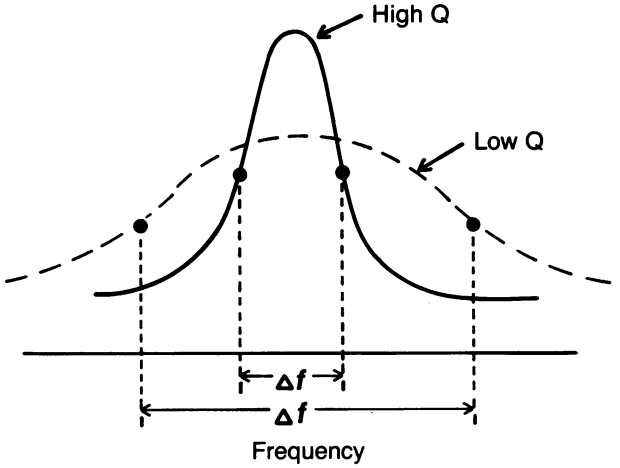

Figure 8.—Dependence of bandwidth, Δf, of coil on value of coil Q.

sources of noise such as mismatching of coil and amplifier impedances and other electronic signal losses.

A significant improvement in coil operation has resulted from decoupling of the transmitter and receiver coils. In an MR imaging unit, the transmitter typically generates high-powered pulses (10 kW), while the receiver coil must be sensitive to microvolt (μV) return signals. By creating two separate coils and positioning them orthogonally to each other, cross talk between the coils can be eliminated and the coils can be individually optimized. Currently, manufacturers are investigating the use of quadrature transmitting and receiving coils as another means of improving sensitivity.[61] In a quadrature coil system, two coils are located orthogonally to each other. Signals in the two coils are phase shifted with respect to each other to reduce noise and the use of two coils increases the signal obtained from the tissue sample.

Perhaps the most exciting coil development has been the use of surface coils to produce high-resolution images of superficial structures such as the spine, orbits, neck and breast.[62-64] Surface coils are typically circular or elliptical in shape and contoured to the body region to be imaged. In this manner the filling factor is increased and noise from other regions of the body is decreased, yielding a higher signal-noise ratio, finer resolution and thinner slices. Penetration of the radio-frequency signal is limited to a depth equal to the coil's radius. In addition, the smaller coils have less homogeneous radio-frequency fields and tissues are not uniformly excited, resulting in nonuniformity of signal intensity in images.

Some nonuniformity can be avoided by decoupling the transmitting and receiving coils. Decoupling typically is accomplished by using the standard head or body coil as the transmitter and the surface coil as the receiver coil. Usually the head or body coil is located farther from the imaged region and irradiates the entire tissue volume inside the coil; hence, more power is deposited in the patient with the decoupling technique. (A surface coil for the spine is shown in Figure 9. Also shown is the difference in resolution and uniformity for a standard body coil compared with the surface coil.)

Siting

Siting considerations depend on both the geometry and the field strength of the magnet. Because of their solenoidal geometry, superconducting and resistive magnets exhibit fringe magnetic fields. The extent of these three-dimensional stray fields depends on the field strength of the magnet. A typical 0.5-tesla magnet has a stray field strength of 5 gauss (G)—1 gauss = 0.0001 tesla—along the magnet axis at a distance of 8 m from the magnet center. This distance increases to 12 m for a 1.5-tesla magnet. Because of these stray magnetic fields, it was originally thought that MR imaging units (especially high field strength units) had to be sited in separate, remote buildings. Subsequently, it has been learned that even high field strength units can be housed in existing facilities by the use of steel enclosures and improved engineering design.[65,66] MR imaging units using permanent magnets do not produce significant fringe magnetic fields.

The interaction between an MR imaging unit and its environment is twofold: the stray magnetic field exerts an influence on the surrounding environment and personnel, and ferromagnetic materials in the environment influence the homogeneity of the magnetic field within the magnet bore. Site planning guides of different vendors vary considerably in their precautions against using electronic equipment around MR imaging units. Magnetic storage media (computer tapes and credit cards) and equipment that relies on electron beams (video monitors and cathode ray tubes) and photomultiplier tubes (CT units and scintillation cameras) can be affected. Little data are available on the intensity thresholds for the effects of magnetic fields on the operation of electronic equipment; in all likelihood, values would vary depending on the design and inherent shielding of the instrument. In general, vendor guidelines are conservative with respect to instrument function, erasing of stored data and so forth; experience to date is inadequate to address effects occurring over a longer term.

Guidelines for the location of ferromagnetic materials near the magnet are also provided in vendor guides. Large masses of stationary ferromagnetic materials can normally be compensated by "shimming" during installation of the MR imaging unit. Transient masses of ferromagnetic materials of any size should not be allowed near the MR imaging unit because they distort the magnetic field; they also could be hazardous if pulled towards the magnet. Large transient ferromagnetic objects, such as automobiles, elevators and trans-

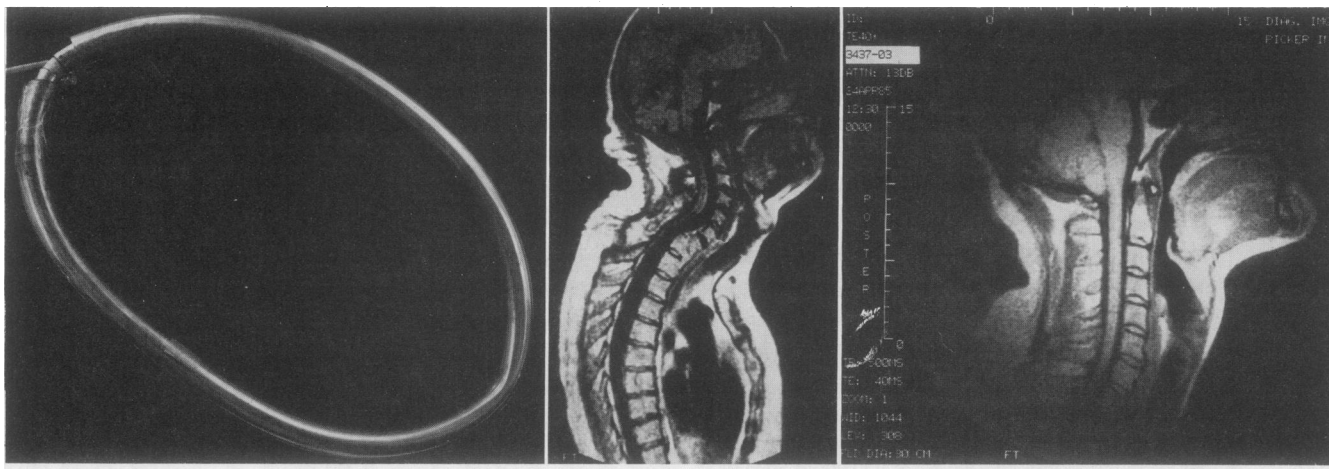

Figure 9.—Left, An elliptical surface coil used for spine imaging. **Middle,** A spine image obtained with a standard body coil. **Right,** A cervical spine image obtained with a surface coil. Note the higher image detail in the region of interest but lower image uniformity. (Photographs courtesy of R. Edward Hendrick, PhD, Department of Radiology, University of Colorado Health Sciences Center.)

port carts, should be kept outside of the 1-gauss field lines to avoid distortion of the magnetic field in the imaging unit.

With regard to steel enclosures for MR imaging units, assorted shielding configurations have been used, including a cylindrical barrel-shaped dome,[67] parallel plates and a rectangular box.[68] One advantage of the box design is that it can also provide radio-frequency shielding. Self-shielded magnets have also been designed[69]; usually these require some additional room shielding to reduce stray fields to levels comparable with those in a shielded facility.

Other major siting considerations include radio-frequency shielding,[70] access route for a superconducting magnet, weight distribution for a permanent magnet and cryogen venting. Most vendors provide detailed guidelines to address these issues. Of course, if permanent siting of an MR imaging system is a problem, mobile units of nearly all available field strengths and magnet types can be purchased.

Safety

Potential bioeffects from MR imaging have been extensively reviewed.[3] Although past studies indicate that there are no harmful bioeffects associated with MR imaging, investigations continue on the premise that negative results do not rule out all possible risks.

In recent studies there was no evidence of damage or genetic aberration of cells at fields up to 2.7 tesla and exposure times up to 17 hours.[71,72] An epidemiologic study of 792 workers at national laboratories exposed to static magnetic fields of 0.5 millitesla to 2 tesla showed no increased incidence in 19 disease classifications.[73]

No change in pineal function was noted during MR imaging of four subjects.[74] The only documented bioeffect was the induction of visual sensations by changing magnetic fields of 1.3 tesla per second at a rate of 15 per second. This effect has been attributed to a torque that alters the shape of retinal rods.[75] No evidence has been reported that this effect is either deleterious or permanent.

Guidelines of the Center for Devices and Radiological Health (formerly the Bureau of Radiological Health) remain as established in 1982.[76] Levels considered safe include static magnetic fields below 2 tesla; time varying fields less than 3 tesla per second and radio-frequency exposures causing specific power absorption rates less than 2 W per kg over 1 gram of tissue and 0.4 W per kg over the entire body. The Food and Drug Administration (FDA) has granted approval to nine commercial systems that adhere to these guidelines. In addition, conditional FDA approval has been awarded to three systems (Table 1). Approval is limited to specific imaging systems and techniques. Any changes in these systems such as increasing field strength or changing imaging protocols require further approval from the FDA.

Although no tissue damage has been shown from MR imaging, there are specific contraindications for an MR imaging examination. The presence of magnetic fields of 17 G or greater has been shown to switch cardiac pacemakers to asynchronous (nondemand mode) operation.[77] These and other electronic implants are susceptible to malfunction due to voltages induced by changing magnetic fields. In addition, radio-frequency pulses of sufficient amplitude and pulse rate can potentially mimic electrical activity of the heart and interfere with the proper operation of cardiac devices. Hence, implant

TABLE 1.—*Magnetic Resonance Imaging Units Approved by the Food and Drug Administration (FDA)*

Vendor	*Field Strength, telsa*
Diasonics Inc	0.35
Fonar	0.3
General Electric Co	0.5, 1.0, 1.5
Picker International Inc—head, neck	0.5
Picker International Inc—body	(0.5)*
Siemens Medical Systems Inc	0.35, 0.5, (1.0)*, (1.5)*
Technicare Corp	0.5

*Recommended for FDA and approved by the FDA Advisory Board.

patients should not be imaged; in fact, they should be excluded from areas where the magnetic field exceeds 5 G. Other contraindications at present include patients who are subject to seizures, claustrophobia, cardiac arrest or who are unconscious or morbidly ill.

Ferromagnetic materials are attracted by magnetic fields and experience a torque causing them to line up with the field. Persons containing such devices should not be imaged by magnetic resonance. In a study of metallic surgical and dental implants, 16 of 21 vascular clips and one shunt connector were found to be affected by MR imaging magnetic fields.[78] Forces on five clips were considered sufficient to dislodge or displace the clip, possibly causing hemorrhage or cerebral injury. Unaffected metallic devices were nonferromagnetic and made from high nickel (10% to 14%) stainless steel, alloys, tantalum or titanium.

At many sites patients with a surgical history are required to provide appropriate medical records or obtain an x-ray examination to document the presence or absence of surgical clips. Only when the radiologist is confident that implants are nonferromagnetic should a person be imaged.

Eye makeup also contains ferromagnetic material that can cause eye irritation during or after imaging. Patients should remove heavy eye makeup before an examination.

Another biological concern of MR imaging arises from its potential to heat metallic implants such as prostheses, surgical clips and intrauterine devices. The heating is caused by electrical currents induced by changing magnetic and radio-frequency fields. Heating effects have not been seen except in one case of two hip prostheses subjected to MR imaging regimens in vitro in a conducting saline solution.[79] In general, patients with metallic implants can be imaged successfully.[80]

Ferromagnetic objects such as pens, scissors, tools and gurneys are attracted to the magnet and should be excluded from the room. The potential for patient injury from these flying objects is probably the chief biohazard of MR imaging. Metal detectors sensitive enough to pick up such objects will also detect nonhazardous objects on MR personnel (belt buckles, jewelry and the like) and thus are relatively ineffective as a screening technique. Usually warning signs and personnel education are sufficient to keep ferromagnetic objects from the examination room.

Wheelchairs and gurneys needed for nonambulatory patients should be nonferromagnetic, such as aluminum. Crash carts are typically ferromagnetic and contain equipment (respirators, defibrillation and so forth) that may not function properly in an intense magnetic field. If emergency resuscitation is required, a typical crash cart should not be brought into

the magnet room. Instead, a core area should be available outside the scan room and a strong nonferromagnetic gurney[81] or removable MR imaging table should be available for rapid transport of the patient to the core area.

MR Field Strength

The optimum field strength for MR imaging is probably the most hotly contested issue among researchers. Resolving this issue is complicated by the marketing strategies of major equipment manufacturers[82] and by the uncertainty of selected clinical applications of magnetic resonance. Questions related to the field strength issue involve image quality (signal-noise ratio, resolution, slice thickness), imaging times, radio-frequency power deposition, spectroscopic applications, cost and siting.

Fundamental to the field strength debate is the fact that the magnetic resonance signal increases with magnetic field strength. As the field strength increases, the energy difference increases between the nuclei aligned with and against the field. Because more energy is required to align against a more intense field, a greater number of nuclei adopt the lower energy state of alignment with the field. This alignment process yields an increase in signal strength because the signal depends on the population difference between the two energy states. Noise also increases with a higher field, but theoretically not so rapidly as the signal. At low fields, noise results mainly from radio-frequency coils and assorted electronics; at higher fields it emanates chiefly from the object being imaged. As a result, the signal-noise ratio can be shown theoretically to increase with magnetic field strength. A higher signal-noise ratio should yield an improved image. In general, researchers agree with this basic tenet, but they argue over the rate of increase of the signal-noise ratio with field strength and whether the improvement in image quality is enough to justify the cost of a higher field magnet.[26,83]

By the same theoretical arguments, proponents of high field systems predict that the contrast-to-noise ratio increases with field strength. The contrast-to-noise ratio is thought to be a very important variable because contrast determines the visibility of tissue structure. Differences in T1 values among tissues, however, decrease with increasing field strength,[84] and this decrease results in a decrease in the contrast-noise ratio.[85,86] High-field proponents counter that T2, which is independent of field strength, has a greater influence on contrast than does T1; hence, the contrast-noise ratio does increase with field strength.[87,88]

Practical advantages of an increased signal-noise or contrast-noise ratio should include improved image quality and thinner slices. A certain level of signal is required from any tissue if an image is to be produced. If the signal can be increased, then one should be able to subdivide the tissue volume and still obtain sufficient signal from each of the small volumes to produce a higher resolution or thinner section image. Some workers say that the signal increase can be accomplished by using higher field systems. Others counter that the image is degraded at higher fields, by the chemical shift effects discussed previously. Two methods for improving resolution are shown in Figure 10. In the first method (Figure 10-A), the resolution element, ΔZ, is decreased by narrowing the bandwidth, Δf, of the radio-frequency signal while the gradient is kept constant. At higher field strengths, this method is not feasible as the fat and water proton peaks are separated too widely. Instead, a technique of increasing the gradient strength is used (Figure 10-B). With this approach, a smaller region, ΔZ_A, can be imaged for the same bandwidth pulse. Noise levels also increase with increasing gradient strength, thereby setting a limit on the available improvement of signal-noise ratio. Proponents of high field systems claim that chemical shift is not a problem in the head, but concede that it may be troublesome in body imaging.[82]

An increase in the signal-noise ratio can also reduce patient examination times by decreasing n, the number of signal averages required to produce sufficient signal-noise ratio in an image. As shown previously, the examination time increases linearly with n, as well as with TR and N. Proponents of low fields claim that a larger TR is needed at high fields because its choice depends on the T1 values of tissues, and T1 has been shown to increase with field strength.[89] In addition, if low field images can be produced at values of $n = 1$, then any possible high field advantage is negated. In fact, imaging will take more time because of increases in TR.

Another influence on imaging time is the increase in radio-frequency power absorption at higher field strength. Power levels can even exceed the guidelines of the Center for Devices and Radiological Health when rapid pulsing schemes required for efficient multislice imaging are used. Power levels can be reduced by decreasing the number of sections

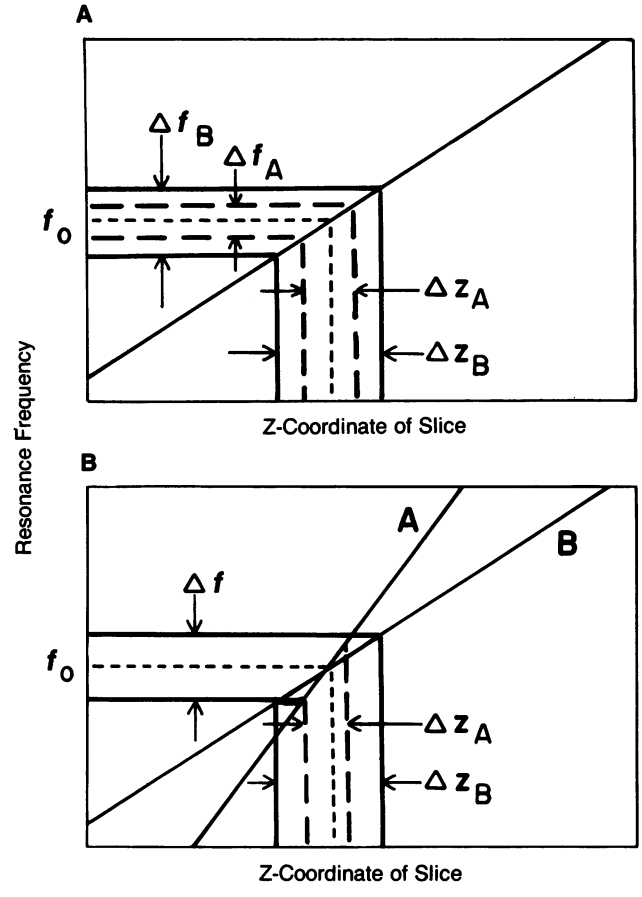

Figure 10.—Techniques for reducing the slice thickness. **A,** The bandwidth Δf_A is narrower than Δf_B, producing a thinner slice thickness ΔZ_A. **B,** The gradient strength A is steeper than B, producing a thinner slice thickness ΔZ_A.

taken simultaneously, but this approach increases examination time. Proponents of high field systems argue that the power deposition guidelines are too low and will eventually be raised.[82]

For spectroscopic studies of nuclei other than hydrogen, there is no question but that high field systems are required. Phosphorus,[90] sodium[91] and fluorine[92] images have been produced at fields of 1.5 to 2 tesla; they yield rather poor spatial resolution images, however, and require long imaging times. Some researchers are investigating fields from 4 to 8 tesla for spectroscopic imaging.

From a purchaser's standpoint, system cost and siting must also be considered as two factors associated with field strength. A higher field system (1.5 to 2 tesla) costs about $1 million more than does a low field (0.6 tesla or less) unit. Although high field units can be sited in existing facilities, the shielded rooms average $500,000. Without question, a potential purchaser of an MR imaging unit needs to be familiar with the many issues associated with controversy over high- and low-field MR imaging units and how these issues relate to the specific intended use of the MR imaging system.

The many technical advances discussed here have yielded appreciable improvement in image quality and clinical utility of MR imaging over the past few years. Many of these improvements are summarized elsewhere in this issue.* This imaging procedure is still in its infancy and there is no reason to believe that the current rate of advancement will not be maintained for several years.

*See "Clinical Applications of Magnetic Resonance Imaging—Current Status" by D. Cammoun, MD; W. R. Hendee, PhD, and K. A. Davis, MD, pp 793-803.

REFERENCES

1. Lauterbur PC: Image formation by induced local interactions: Examples employing nuclear magnetic resonance. Nature 1973; 242:190-191

2. 200 MRI Systems on-line in U.S. and abroad by January 1 (Business Briefs). Diagn Imaging 1984 Nov, pp 64-70

3. Hendee WR, Morgan CJ: Magnetic resonance imaging: Part I—Physical principles (Medical Progress). West J Med 1984 Oct; 141:491-500

4. Pykett IL: NMR imaging in medicine. Sci Am 1982; 246:78-88

5. Newton TH, Potts DG (Eds): Modern Neuroradiology, Vol II—Advanced Imaging Techniques. San Anselmo, Calif, Clavadel Press, 1983

6. Wehrli FW, MacFall JR, Glover GH, et al: The dependence of nuclear magnetic resonance (NMR) image contrast on intrinsic and pulse sequence timing parameters. Magn Reson Imaging 1984; 2:3-16

7. Hendrick RE, Nelson TR, Hendee WR: Optimizing tissue contrast in magnetic resonance imaging. Magn Reson Imaging 1984; 2:193-204

8. Brant-Zawadzki M, Norman D, Newton TH, et al: Magnetic resonance of the brain: The optimal screening technique. Radiology 1984; 152:71-77

9. Ortendahl DA, Hylton N, Kaufman L, et al: Analytical tools for magnetic resonance imaging. Radiology 1984; 153:479-488

10. Riederer SJ, Suddarth SA, Bobman SA, et al: Automated MR image synthesis: Feasibility studies. Radiology 1984; 153:203-206

11. Smith SD, Kranzer HC, Gusack RK: Intensity and contrast profiles in multislice NMR imaging, abstract No. 45. Abstracts of the Third Annual Meeting of the Society for Magnetic Resonance Imaging, San Diego, Mar 1985

12. Wehrli FW, MacFall JR, Newton TH: Parameters determining the appearance of NMR images. *In* Newton TH, Potts DG (Eds): Modern Neuroradiology, Vol II—Advanced Imaging Techniques. San Anselmo, Calif, Clavadel Press, 1983, pp 81-117

13. Crooks LE, Watts J, Hoenninger J, et al: Thin-section definition in magnetic resonance imaging. Radiology 1985; 154:463-467

14. Crooks LE, Barker B, Chang H, et al: Magnetic resonance imaging strategies for heart studies. Radiology 1984; 153:459-465

15. Soila KP, Viamonte M Jr, Starewicz PM: Chemical shift misregistration effect in magnetic resonance imaging. Radiology 1984; 153:819-820

16. Pykett IL, Rosen BR: Nuclear magnetic resonance: In vivo proton chemical shift imaging. Radiology 1983; 149:197-201

17. Scott KN, Marece TH: Enhanced fat-water contrast imaging at 0.15 T, abstract. Abstracts of the Third Annual Meeting of the Society of Magnetic Resonance in Medicine, August 1984, New York. Berkeley, Calif, Society of Magnetic Resonance in Medicine, 1984, pp 668-669

18. Dixon WT: Simple proton spectroscopic imaging. Radiology 1984; 153:189-194

19. Bottomley PA, Foster TH, Leue WM: ^{1}H chemical shift imaging of the brain, abstract. Abstracts of the Third Annual Meeting of the Society of Magnetic Resonance in Medicine, August 1984, New York. Berkeley, Calif, Society of Magnetic Resonance in Medicine, 1984, pp 72-73

20. Lee JK, Dixon WT, Ling D, et al: Fatty infiltration of the liver: Demonstration by proton spectroscopic imaging. Radiology 1984; 153:195-201

21. Mills CM, Brant-Zawadzki M, Crooks LE, et al: Nuclear magnetic resonance: Principles of blood flow imaging. AJR 1983; 4:1161-1166

22. Bradley WG, Waluch V: Blood flow: Magnetic resonance imaging. Radiology 1985; 154:443-450

23. Singer JR, Crooks LE: Nuclear magnetic resonance blood flow measurements in the human brain. Science 1983; 221:654-656

24. Moran PR: Verification and evaluation of internal flow and motion. Radiology 1985; 154:433-441

25. O'Donnell M: NMR blood flow imaging using multiecho phase contrast sequences. Med Phys 1985; 12:59-64

26. Crooks LE, Arakawa M, Hoenninger JC, et al: Magnetic resonance imaging: Effects of magnetic field strength. Radiology 1984; 151:127-133

27. Edelstein WA: Signal and noise considerations in NMR imaging and spectroscopy. Abstracts of the Third Annual Meeting of the Society of Magnetic Resonance in Medicine, August 1984, New York. Berkeley, Calif, Society of Magnetic Resonance in Medicine, 1984, p 202

28. Dinsmore RE, Wismer GL, Levine RA, et al: Magnetic resonance imaging of the heart: Positioning and gradient angle selection for optimal imaging planes. AJR 1984; 143:1135-1142

29. Murphy WA, Gutierrez FR, Levitt RG, et al: Oblique views of the heart by magnetic resonance imaging. Radiology 1985; 154:225-226

30. Feiglin DH, George CR, MacIntyre WJ, et al: Gated cardiac magnetic resonance structural imaging: Optimization by electronic axial rotation. Radiology 1985; 154:129-132

31. Runge VM, Clanton JA, Partain CL, et al: Respiratory gating in magnetic resonance imaging at 0.5 tesla. Radiology 1984; 151:521-523

32. Mansfield P, Pykett IL: Biological and medical imaging by NMR. J Magn Reson 1978; 29:355-373

33. Mansfield P: Echo-planar MR imaging. Radiol Nucl Med Images. 1984; 14:22-25

34. Damadian R: Tumor detection by nuclear magnetic resonance. Science 1971; 171:1151-1153

35. Araki T, Inouye T, Suzuki H, et al: Magnetic resonance imaging of brain tumors: Measurement of T1. Radiology 1984; 150:95-98

36. Mills CM, Crooks LE, Kaufman L, et al: Cerebral abnormalities: Use of calculated T1 and T2 magnetic resonance images for diagnosis. Radiology 1984; 150:87-94

37. Bernardino ME, Small W, Goldstein J, et al: Multiple NMR T2 relaxation values in human liver tissue. AJR 1983; 141:1203-1208

38. Rosen BR, Pykett IL, Brady TJ: Spin lattice relaxation time measurements in two-dimensional nuclear magnetic resonance imaging: Corrections for plane selection and pulse sequence. J Comput Assist Tomogr 1984; 8:195-199

39. Lin MS: Accuracy of proton T1 calculated by approximations from image signals. J Nucl Med 1985; 26:54-58

40. Kjos BO, Ehman RL, Brant-Zawadzki M, et al: Reproducibility of relaxation times and spin density calculated from routine MR imaging sequences: Clinical study of CNS. AJNR 1985; 6:271-276

41. Kjos BO, Ehman RL, Brant-Zawadzki M: Reproducibility of T1 and T2 relaxation times calculated from routine MR imaging sequences: Phantom study. AJNR 1985; 6:277-283

42. Brasch RC: Work in Progress: Methods of contrast enhancement for NMR imaging and potential applications. Radiology 1983; 147:781-788

43. Runge VM, Clanton JA, Lukehart CM, et al: Paramagnetic agents for contrast-enhanced NMR imaging: A review. AJR 1983; 141:1209-1215

44. Wolf GL, Baum L: Cardiovascular toxicity and tissue proton T1 response to manganese injection in the dog and rabbit. AJR 1983; 141:193-197

45. Slutsky RA, Peterson T, Strich G, et al: Hemodynamic effects of rapid and slow infusions of manganese chloride and gadolinium-DTPA in dogs. Radiology 1985; 154:733-735

46. Wolf GL, Burnett KR, Goldstein EJ, et al: Contrast agents for magnetic resonance imaging, *In* Kressel HY (Ed): Magnetic Resonance Annual. New York, Raven Press, 1985, pp 231-266

47. Wesbey GE, Brasch RC, Engelstad BL, et al: Nuclear magnetic resonance contrast enhancement study of the gastrointestinal tract of rats and a human volunteer using nontoxic oral iron solutions. Radiology 1983; 149:175-180

48. Lauffer RB, Greif L, Stark DD, et al: Iron-EHPG as an hepatobiliary MR contrast agent: Initial imaging and biodistribution studies. J Comput Assist Tomogr 1985; 3:431-438

49. Weinmann HJ, Brasch RC, Press WR, et al: Characteristics of gadolinium-DTPA complex: A potential MRI contrast agent. AJR 1984; 142:619-624

50. Gadian DG, Payne JA, Bryant DJ, et al: Gadolinium-DTPA as a contrast agent in MR imaging—Theoretical projections and practical observations. J Comput Assist Tomogr 1985; 9:242-251

51. Strich G, Hagan PL, Gerber KH, et al: Tissue distribution and magnetic resonance spin lattice relaxation effects of gadolinium-DTPA. Radiology 1985; 154:723-726

52. Vinocur B: MRI contrast agents: Can they enhance specificity? Diagn Imaging 1984 Sep, pp 54-61

53. Carr DH, Brown J, Bydder GM, et al: Gadolinium-DTPA as a contrast agent in MRI: Initial clinical experience in 20 patients. AJR 1984; 143:215-224

54. Grossman RI, Wolf G, Biery D, et al: Gadolinium enhanced nuclear magnetic

resonance images of experimental brain abscess. J Comput Assist Tomogr 1984; 8:204-207

55. McNamara MT, Higgins CB, Ehman RL, et al: Acute myocardial ischemia: Magnetic resonance contrast enhancement with gadolinium-DTPA. Radiology 1984; 153:157-163

56. Wesby GE, Higgins CB, McNamara MT, et al: Effect of gadolinium-DTPA on the magnetic relaxation times of normal and infarcted myocardium. Radiology 1984; 153:165-169

57. Brasch RC, London DA, Wesbey GE, et al: Work in Progress: Nuclear magnetic resonance study of a paramagnetic nitroxide contrast agent for enhancement of renal structures in experimental animals. Radiology 1983; 147:773-779

58. Brasch RC, Nitecki DE, Brant-Zawadzki M, et al: Brain nuclear magnetic resonance imaging enhanced by a paramagnetic nitroxide contrast agent: Preliminary report. AJR 1983; 141:1019-1023

59. Jones JP, Partain CL, Mitchell MR, et al: Principles of magnetic resonance, *In* Kressel HY (Ed): Magnetic Resonance Annual. New York, Raven Press, 1985, pp 71-111

60. Hoult DI: Radiofrequency coil technology in NMR scanning. Proceedings of an International Symposium on Nuclear Magnetic Resonance Imaging. Winston-Salem, NC, Bowman Gray School of Medicine of Wake Forest Univ, 1981, pp 33-39

61. Sank VJ, Chen CN, Hoult DI: A quadrature probe for adult head NMR imaging. Abstracts of the Third Annual Meeting of the Society of Magnetic Resonance in Medicine, August 1984, New York. Berkeley, Calif, Society of Magnetic Resonance in Medicine, 1984, p 650

62. Ackerman JJH, Grove TH, Wong GG, et al: Mapping of metabolites in whole animals by ^{31}P NMR using surface coils. Nature 1980; 283:167-170

63. Ampara EG, Brandt G, Brant-Zawadzki MN, et al: MR imaging using surface coils. Radiology 1984; 153:243 [RSNA abstracts]

64. Fitzsimmons JR, Thomas RG, Mancuso AA: Communication: Proton imaging with surface coils on a 0.15-T resistive system. Magn Reson Med 1985; 2:180-185

65. Peters C, Proseus J: MRI siting in adverse environments—Experimental results, I. Abstracts of the Third Annual Meeting of the Society of Magnetic Resonance in Medicine, August 1984, New York. Berkeley, Calif, Society of Magnetic Resonance in Medicine, 1984, p 585

66. Eqing JR, Timms W, Helpern J, et al: Magnetic shielding and site planning for a large-bore, high field magnet. Abstracts of the Third Annual Meeting of the Society of Magnetic Resonance in Medicine, August 1984, New York. Berkeley, Calif, Society of Magnetic Resonance in Medicine, 1984, p 224

67. Den Boer JA, Vreugdehil E: Hybrid shielding of the static magnetic stray field generated by a 0.5 T whole body NMR system. Abstracts of the Third Annual Meeting of the Society of Magnetic Resonance in Medicine, August 1984, New York. Berkeley, Calif, Society of Magnetic Resonance in Medicine, 1984, p 188

68. Kalafala AK, Varrek RM: Magnetic shields for MR magnets. Abstracts of the Third Annual Meeting, Society for Magnetic Resonance Imaging, March 1985, San Diego. McClean, VA, Society for Magnetic Resonance Imaging, 1985, p 71

69. Ries G, Frese G, Siemens A: Magnetic shielding of whole body MR-magnets. Abstracts of the Third Annual Meeting of the Society of Magnetic Resonance in Medicine, August 1984, New York. Berkeley, Calif, Society of Magnetic Resonance in Medicine, 1984, p 625

70. Graham J: RF shielding for NMR images, *In* Esser P, Johnston RE (Eds): Technology of Nuclear Magnetic Resonance. New York, The Society of Nuclear Medicine, 1984, pp 2523-2527

71. Wolff S, James TL, Young GB, et al: Magnetic resonance imaging: Absence of in vitro cytogenetic damage. Radiology 1985; 155:163-165

72. Geard CR, Osmak RS, Hall EJ, et al: Magnetic resonance and ionizing radiation: A comparative evaluation in vitro of oncogenic and genotoxic potential. Radiology 1984; 152:199-202

73. Budinger TF, Bristol KS, Yen CK, et al: Biological effects of static magnetic fields. Abstracts of the Third Annual Meeting of the Society of Magnetic Resonance in Medicine, August 1984, New York. Berkeley, Calif, Society of Magnetic Resonance in Medicine, 1984, p 113

74. Prato FS, Kavaliers M, Ossenkopp KP, et al: Exposure to NMR imaging fails to depress nocturnal serum melatonin levels in male humans. Abstracts of the Third Annual Meeting of the Society of Magnetic Resonance in Medicine, August 1984, New York. Berkeley, Calif, Society of Magnetic Resonance in Medicine, 1984, p 598

75. Budinger TF, Cullander C, Bordow R: Switched magnetic field thresholds for the induction of magnetophosphenes. Abstracts of the Third Annual Meeting of the Society for Magnetic Resonance in Medicine, August 1984, New York. Berkeley, Calif, Society of Magnetic Resonance in Medicine, 1984, p 118

76. Food and Drug Administration: Guidelines for Evaluation of Electromagnetic Exposure Risk for Trials of Clinical NMR Systems. Rockville, Md, Dept Health and Human Services, 1982

77. Pavlicek W, Geisinger M, Castle L, et al: The effects of nuclear magnetic resonance on patients with cardiac pacemakers. Radiology 1983; 147:149-153

78. New PF, Rosen BR, Brady TJ, et al: Potential hazards and artifacts of ferromagnetic and nonferromagnetic surgical and dental materials and devices in nuclear magnetic resonance imaging. Radiology 1983; 147:139-148

79. Davis PL, Crooks L, Arakawa M, et al: Potential hazards in NMR imaging: Heating effects of changing magnetic fields and RF fields on small metallic implants. AJR 1981; 137:857-860

80. Mechlin M, Thickman D, Kressel HY, et al: Magnetic resonance imaging of postoperative patients with metallic implants. AJR 1984; 143:1281-1284

81. Weinreb JC, Marawella KR, Peshock P, et al: Magnetic resonance imaging: Improving patient tolerance and safety. AJR 1984; 143:1285-1287

82. Vinocur B: MR magnet strength debate: In search of an optimum field. Diagn Imaging 1984 Nov, pp 106-113

83. Hoult DI, Lauterbur PC: The sensitivity of the zeugmatographic experiment involving human samples. J Magn Reson 1979; 34:425-433

84. Beall PT, Amtey SR, Kasturi SR: NMR Data Handbook for Biomedical Applications. New York, Pergamon Press, 1984

85. Kaufman L, Crooks L, Margulis A: MRI at the threshold. Diagn Imaging 1984, pp 36-43

86. Chen GN, Sank VJ, Hoult DI: Probing image frequency dependence. Abstracts of the Third Annual Meeting of the Society of Magnetic Resonance in Medicine, August 1984, New York. Berkeley, Calif, Society of Magnetic Resonance in Medicine, 1984, pp 148-152

87. Bottomley PA, Hart HR Jr, Edelstein WA, et al: Anatomy and metabolism of the normal human brain studied by magnetic resonance at 1.5 tesla. Radiology 1984; 150:441-446

88. Hart HR Jr, Bottomley PA, Edelstein WA, et al: Nuclear magnetic resonance imaging: Contrast-to-noise ratio as a function of strength of magnetic field. AJR 1983; 141:1195-1201

89. Fullerton GD, Cameron IL, Ord VA: Frequency dependence of magnetic resonance spin-lattice relaxation of protons in biological materials. Radiology 1984; 151:135-138

90. Maudsley AA, Hilal SK, Simon HE, et al: In vivo MR spectroscopic imaging with P-31. Radiology 1984; 153:745-750

91. Hilal SK, Lee S, Cho ZH, et al: Proton and sodium NMR in stroke. Abstracts of the Third Annual Meeting of the Society of Magnetic Resonance in Medicine, August 1984, New York. Berkeley, Calif, Society of Magnetic Resonance in Medicine, 1984, p 323

92. Horner SD, Babcock EE, Nunnally RL: Evaluation of myocardial perfusion by ^{19}F NMR imaging. Abstracts of the Third Annual Meeting of the Society of Magnetic Resonance in Medicine, August 1984, New York. Berkeley, Calif, Society of Magnetic Resonance in Medicine, 1984, pp 338-339